ORIGINAL PAPER

Lighting up ATP in cells and tissues using a simple aptamer-based fluorescent probe

Wenjun Liu[1] · Xuena Zhu[2,3] · Maedeh Mozneb[3] · Larry Nagahara[4] · Tony Y. Hu[5] · Chen-Zhong Li[3,5]

Abstract

Extracellular ATP as a purinergic signaling molecule, together with ATP receptor, are playing an important role in tumor growth, therapy resistance, and host immunity suppression. Meanwhile ATP is a crucial indicator for cellular energy status and viability, thus a vital variable for tissue regeneration and in vitro tissue engineering. Most recent studies on COVID-19 virus suggest infection caused ATP deficit and release as a major characterization at the early stage of the disease and major causes for disease complications. Thus, imaging ATP molecule in both cellular and extracellular contexts has many applications in biology, engineering, and clinics. A sensitive and selective fluorescence "signal-on" probe for ATP detection was constructed, based on the base recognition between a black hole quencher (BHQ)-labeled aptamer oligonucleotide and a fluorophore (Cy5)-labeled reporter flare. The probe was able to detect ATP in solution with single digit μM detection limit. With the assistance of lipofectamine, this probe efficiently entered and shined in the model cells U2OS within 3 h. Further application of the probe in specific scenery, cardio-tissue engineering, was also tested where the ATP aptamer complex was able to sense cellular ATP status in a semi-quantitative manner, representing a novel approach for selection of functional cardiomyocytes for tissue engineering. At last a slight change in probe configuration in which a flexible intermolecular A14 linker was introduced granted regeneration capability. These data support the application of this probe in multiple circumstances where ATP measurement or imaging is on demand.

Keywords Fluorescent probe · Aptamer · ATP · Live cell imaging · Cardiac tissue engineering · COVID-19

Introduction

Among many metabolites, ATP is majorly produced in mitochondria and resides in cells with a concentration of 5–10 mM. Intracellular ATP represents the principal source of cellular energy and is indicative for cell energy status and viability. It is shown to be crucial for in vivo tissue repair/regeneration and in vitro tissue engineering [1]. On the other hand, extracellular ATP functions as a pivotal signaling mediator [2–4]. Under normal physiological conditions, ATP is barely detectable in extracellular contents. ATP is

Wenjun Liu and Xuena Zhu contributed equally to this work.

✉ Xuena Zhu
xzhu09@zju.edu.cn

✉ Tony Y. Hu
tonyhu@tulane.edu

✉ Chen-Zhong Li
chenzhongbiosensor@gmail.com

1   Zhejiang Provincial Key Laboratory of Pancreatic Disease and Department of Hepatobiliary and Pancreatic Surgery, the First Affiliated Hospital, Zhejiang University School of Medicine, Hangzhou 310002, Zhejiang, China

2   Department of Pathology, the First Affiliated Hospital and School of Medicine, Zhejiang University, Hangzhou 310002, Zhejiang, China

3   Nanobioengineering/Bioelectronics Laboratory, Department of Biomedical Engineering, Florida International University, 10555 West Flagler Street, Miami, FL 33174, USA

4   Department of Chemical and Biomolecular Engineering, Whiting School of Engineering, Johns Hopkins University, Baltimore, MD 21218, USA

5   Center for Cellular and Molecular Diagnostics, Department of Biochemistry and Molecular Biology, Tulane University School of Medicine, New Orleans, LA 70112, USA

profoundly released from cells upon mechanical injury and other stimulus [5, 6]. ATP enrichment is widely found in tumor microenvironment at up to tens to hundreds of micromolar [7]. ATP and adenosine arised from the hydrolysis of ATP by membrane bound phosphohydrolase CD73 and CD39 are the major purinergic signaling molecules that pose significant influence on the tumor-host interaction, thus contributing to enhanced immunosuppression, tumor growth, and invasion [8–10].

Most recent research revealed that SARS-CoV2 virus (COVID-19) infection causes cellular ATP deficit [11, 12] and ATP release from infected cells, which, dependently on the site of infection, in turn signals unproductive response at lung [13] or leads to neuroinflammation caused complications [14]. For these considerations, a reliable, safe, and live imaging compatible ATP probing system can be conceivably beneficial for laboratory research, engineered tissue growth in vitro, and patient care on clinical sites.

In situ bioimaging has become a powerful tool in bioanalysis [15–18]. Significant progress has been achieved in the sensing and imaging of metabolites in biological samples containing live cells and tissue [19–21]. Until now, diverse methods have been developed to detect ATP, such as traditional approaches (HPLC, NMR spectroscopy [22], capillary electrophoresis [23]), optical sensors (colorimetric assays [24], fluorometric sensors [25], bioluminescence, and chemiluminescence detection platforms [26]), and electrochemical detection methods [26]. However, new testing that is straightforward, bio-friendly, and live imaging compatible remains on demand.

Over the years, a large repository of nucleic acid-based aptamers that possess biomolecular specificity has been selected and reported. Along with it, extensive efforts have been spent on developing aptamer-based sensors ("aptasensors") for the detection of adenosine, ATP [27], cocaine [28], Hg^{2+} [29], toxins [30], thrombin, vascular endothelial growth factor (VEGF) [31], etc. In the sensing process, aptamers often bind to their targets by a mechanism in which they undergo considerable conformational changes that can be used for converting the binding event into a measurable signal. Combined with various transducers, multiple sensing strategies have been developed, such as fluorescence, colorimetry, electrophoresis, electrochemistry, electrochemiluminescence (ECL), quartz crystal microbalance (QCM), and surface plasmon resonance (SPR) [32–34]. Through direct modification with fluorophores, the conformational changes of aptamers can affect the fluorescence of a dye or the fluorescence resonance energy transfer (FRET) between two dyes. The signal change, either increase (i.e., the "signal-on" mode) or decrease (i.e., the "signal-off" mode), reflects the extent of the binding process, thereby allowing for quantitative measurement of target concentration. Fluorescent molecular probes have so far been playing a major

role for intracellular sensing and imaging [35, 36]. Their fast response, intense signal, relatively low intrinsic cell autofluorescence, and relatively simple instrumental set-up have made fluorescence coupled molecular probe a perfect match for real time measurements in cells.

In this manuscript, we report an easy to fabricate "signal-on" fluorescent probe for ATP detection, which is based on hybridization between a black hole quencher (BHQ)-labeled aptamer oligonucleotide and a fluorophore (Cy5)-labeled reporter flare. This simple design functions stand-alone and is free of bulky attachment such as protein enzyme or nanoparticles. Oligonucleotides undergo clearance by both endonucleases and exonucleases in nucleus and cytosol after extended cellular retainment and thus render minimal interference to cell physiology. Cell friendly excitation and emission of red fluorophore represent another advantage of this probe for cellular application. We demonstrate that the probe is of high selectivity and low detection limit for analytical use in solution. In addition, the feasibility of the probe to be used in cellular context is demonstrated by probing intracellular ATP in U2OS cells as well as in neonatal rat cardiomyocytes.

Materials and methods

Chemicals and materials

Adenosine 5′-triphosphate (ATP), guanosine 5′-triphosphate (GTP), uridine 5′-triphosphate (UTP), cytidine 5′-triphosphate (CTP), and oligomycin were purchased from Sigma-Aldrich (St Louis, MO, USA). Imaging compatible Nunc™ Lab-Tek™ II 8-well chamber slides (Cat#: 155409PK), Hoechst 33,342 (Cat#: H3570), Tubulin Tracker™ Green (Oregon Green™ 488 Taxol, Cat#: T34075), neonatal rat cardiomyocyte isolation enzymes, supplements, and primary cell isolation medias were purchased form Thermo Fisher Scientific (Waltham, MA). Neonatal rat hearts were generously donated from FIU's animal facility. All the other chemicals were of analytical reagent grade and were used as received without further purification.

Preparation of aptamer-based ATP probe

The BHQ-labeled ATP aptamer (5′-ACCTGGGGGAGT ATTGCGGAGGAAGGTGTCACA-BHQ-3′) Cy5-labeled reporter oligo (5′-Cy5-TGTGACACCTTCCT-3′) (Fig. 1) and the modified probe with A14 linker (Fig. 6A) were synthesized by Integrated DNA Technologies (Coralville, IOWA, USA). A 20 μL black hole quencher (BHQ) (100 μM) labeled aptamer oligonucleotides were mixed with 20 μL fluorophore (Cy5)-labeled reporter strands (100 μM) (1:1) in 40 μL 1X PBS (total: 80 μL), heated to 80 °C, slowly

Fig. 1 Design and detection mechanism of aptamer-based ATP probes. The probe comprises of two elements, a 3′ black hole quencher (BHQ) attached ATP aptamer (ssDNA) and a 5′ Cy5 labeled reporter strand. The strands hybridize and present the fluorophore at quenched state when ATP is absent. When ATP incorporates into the molecule complex, conformational change occurs at the aptamer that allows invasion of 5′ end, partial hybridization with 3′ end, and displacement of the reporter flares

Aptamer: 5' - ACCTGGGGGAGTATTGCGGAGGAAGGTGTCACA - BHQ-3'
Reporter: 3'- TCC TTCC ACAGTGT - Cy5-5'
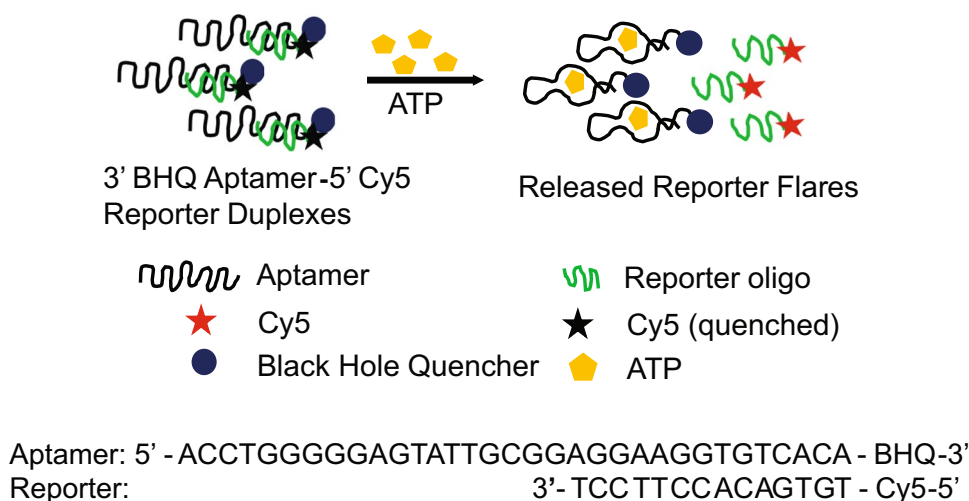
cooled to room temperature, and stored in the dark for overnight allowing efficient hybridization. These stock ATP probes (25 μM) were stored in the refrigerate (4 °C) and dark before use.

Fluorescence studies in solution

Aptamer probes were diluted to a concentration of 250 nM or indicated in 1X PBS. All of the fluorescence spectra were recorded in room temperature immediately after mixing 100 μL diluted probes and ATP samples on a Jasco FP-6500 fluorescence spectrometer with excitation at 633 nm and emission from 650 to 750 nm in 1 nm increments. Optimum temperature for this assessment has not been evaluated. Fluorescence response emerges immediately post-manual mixing, which takes about 2 s, and keeps relatively steady within a 2-h time window. Concentration of the aptamer probe in final reaction can be adjusted to accommodate analytes of different concentration ranges, e.g., 250 nM probe for 1–100 uM ATP and 2 μM probe for 0.1–3 mM ATP. The regeneration study was carried out particularly in nuclease free water and 1X Apyrase buffer that contain calcium.

Gel electrophoresis and detection by fluorescence

Fifteen percent native polyacrylamide gels were employed to separate aptamer duplex and free reporter flare based on their difference in mobility. The casting includes 1X TAE, 15% acrylamide/Bis 29:1, 50 μL 10% ammonium persulfate (APS), and 5 μL tetramethylethylenediamine (TEMED) for each gel (6 mL). Electrophoresis was done within miniprotean electrophoresis system. Images were recorded with BioRad ChemiDoc Imaging System by using its Cy5 fluorescence channel. For visualization of release of the Cy5-labeled reporter flare in response to ATP by polyacrylamide gel electrophoresis, black hole BHQ quencher was excluded

so that the Cy5 fluorescence can be used to trace both free reporter flare and assembled aptamer duplex. A 15 μL reaction (Fig. 2D, lanes 3–7) and 3.75 nmol (Fig. 2D, lane 1–2) were loaded for each lane which suffices the detection limit of the ChemiDoc system. The PAGE was run at the voltage of 20 V for 90 min.

U2OS cell culture and imaging

U2OS cells were incubated in DMEM supplemented with 10% (v/v) fetal bovine serum and 1% (w/v) penicillin/streptomycin at 37 °C in the presence of 5% CO_2 in a benchtop incubator. Cells were passaged when they are approximately 80% confluence. Then, the cells were seeded in a Nunc™ Lab-Tek™ II 8-well chamber slide at a density of 10^4 per well and total media volume 300 μL. After 24 h, the cells were washed with PBS and replenished with fresh media. A 75 μL probes/lipofectamine complex was added to each well. Two hours after adding probes, the cells were washed once with PBS, replenished with fresh media, and subjected to fluorescence microscopic studies. Counterstaining was done by adding tubulin tracker green and Hoechst at final concentration of 0.3 μg/mL and 5 μg/mL respectively, 30 min before washing. Oligomycin at the final concentration of 10 μg/mL was added to cells 2 h in prior to probes. Images from green, red, and blue channels were separately shot with 40× magnitude. Quantification and stacks were prepared with ImageJ.

Cardiomyocyte isolation, culture, and imaging

Neonatal rat cardiomyocytes were isolated following Thermos Fisher Scientific isolation protocol from newborn (1 ~ 2 day old) rat pups. Briefly, the neonatal rats were euthanized via decapitation, and their hearts' ventricles were excised. Each ventricle was immediately put in a

Fig. 2 The ATP probe responses to ATP in a specific and sensitive manner. **A** Solution fluorescence spectra of the aptamer-based probe treated with 100 μM ATP, UTP, GTP, CTP, and AMP. **B** Fluorescence spectra of the aptamer-based ATP probe in solution with increasing concentrations of ATP (0–480 μM). Note: plotted in (**A**) and (**B**) are averages of experimental triplicates. **C** The peak intensity as a function of ATP concentration. **D** Visualization of release of the Cy5-labeled reporter flare in response to ATP by polyacrylamide gel electrophoresis and fluorescence imaging. Black hole quencher was excluded to allow detection of the duplex configuration. A 250 nM preformed aptamer-reporter flare duplex was exposed to serially diluted ATP and GTP (0, 16, 50, 150, and 450 μM; lanes 3–7), which gave rise to low-position (high mobility) bands that correspond to the free Cy5-labeled reporter flare
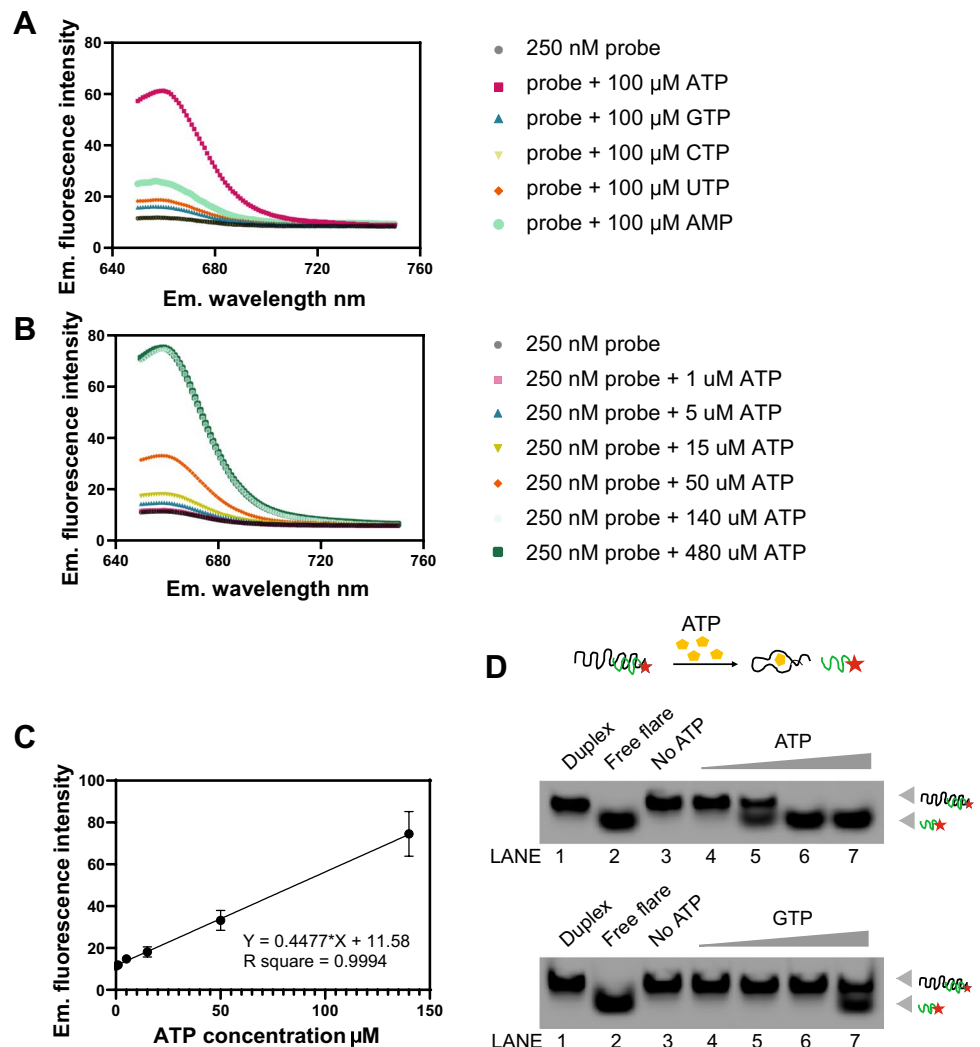
separate 1.5-mL vial filled with ice cold HBSS. They were then trimmed into small pieces (1–3 mm^2) with surgical scissors. A 0.2 mL reconstituted cardiomyocyte isolation enzyme 1 (papain) in HBSS and 10 μL cardiomyocyte isolation enzyme 2 (thermolysin) were added into each tube to digest the cardiac tissue. Vials were incubated in a benchtop incubator (37 °C and 5% CO$_2$) for 35 min. The digests were then collected, and complete DMEM (with 1% penicillin/streptomycin, 10% fetal bovine serum (FBS)) was added to each vial to stop enzyme activity. By using a 1000-unit pipette, the tissue was broken up (pipetting up and down for 30 times until tissue was a single-cell suspension). The vials were combined for cell concentration and viability determination. Finally, the cells were seeded in an 8-well chamber slide at a density of 10^4 cells per well with complete DMEM for primary cell isolation (total media volume 300 μL). After 24 h, the complete DMEM was substituted with media containing cardiomyocytes growth supplement, for cardiomyocyte purification over fibroblasts and endothelial cells. After this, the medium was changed every 3 days. At

day 7, the isolated cardiomyocyte was matured enough for following experiments. Staining of aptamer probes, tubulin tracker green, and Hoechst were done in the same way as for U2OS cells.

ATP sensor enters cells with the assistant of lipofectamine

Cellular delivery of ATP sensor is mediated by lipofectamine. The positive surface charge of the liposomes mediates the interaction of the oligonucleotide and the cell membrane, allowing for fusion of the liposome/oligonucleotide transfection complex with the negatively charged cell membrane and thus successful entry of ATP sensors. In brief, equal volume of diluted probe (0.33 μM) in serum-free media and 1.25% lipofectamine diluted in serum-free median was mixed to form the probe/lipofectamine complex. This sensing complex was added to cell culture (in 1:4 ratio) 30 min after mixing.

Flow cytometry

For flow cytometry studies, cells were seeded in 24 well plates at 50 k/well. The next day, 100 µL probe/lipo-fectamine complex or vehicle control was added into 400 µL culture media. After 2 h incubation in 37 °C, cells were washed with 1X PBS, trypsinized and resuspended in 500 µL complete media, and transferred to flow cytometry sample tubes. Samples were subjected to BD FACS Canto-II analysis immediately with configuration ex 640 nm, em 660/20 nm for Cy5 resolution. Time course evaluation was carried out at 0, 0.5, 1, 2, 3 h post addition of probe/lipo-fectamine complex. It was determined that 2 h incubation be used for other flow and imaging studies. Specificity of the probes to cellular ATP was verified with preceding 2 h of 1 µg/mL oligomycin treatment.

Results and discussion

ATP-specific aptamer-based fluorescence probe exhibits high sensitivity and broad detection range in solution

As illustrated in Fig. 1, our aptamer-based ATP probe duplex is composed of a 3′ BHQ-labeled single strand DNA aptamer and a 5′ Cy5-labeled reporter strand representing an extremely simple design. With the presence of ATP molecules, the aptamer strand undergoes conformation change that facilitates self-annealing of its 5′ and 3′ ends and along with it the displacement of the reporter flare. The release of reporter flare is detected by a fluorometer for quantification of ATP abundance.

Aptamer-based probe duplexes showed a significant fluorescence increase upon target addition. For 250 nM probe, when 100 µM ATP was added, an immediate 6.56-fold increase in fluorescent signal was observed (Fig. 2A). Conversely, addition of the ATP analogues guanidine triphosphate (GTP), cytosine triphosphate (CTP), or uridine triphosphate (UTP) at 100 µM did not result in a significant increase in fluorescent signal when compared to 100 µM ATP (Fig. 2A). Adenosine monophosphate (AMP) results in the largest fluorescence increase among these analogues. These results are consistent with a selective target binding ability of the aptamer probe toward adenosine, and the probe is most responsive to ATP.

The effect of target concentration was also investigated. Probe duplexes (250 nM) responded to the presence of ATP in a dose-dependent manner (Fig. 2B) with a linear range up to 140 µM ATP (Fig. 2C) demonstrating that the fluorescence can be used to quantify ATP concentration in solution. Native polyacrylamide gels were utilized to resolve each reaction species (Fig. 2D). With an aptamer chain that does not contain BHQ group, Cy5 fluorescence assisted in identifying of both assembled probe (lane 1) and free reporter flare (lane 2). ATP concentration-dependent dissociation of the reporter flares from assembly was reproduced on native PAGE as well (lanes 3–7).

Meanwhile, the detection range of the probe in solution can be probe concentration dependent. It is capable of sensing high concentration ATP by simply increasing the concentration of the probe. For instance, the probe at the concentration of 2 µM was responsible to ATP at hundreds µM to single digit mM (Fig. S1). The broad detection limit (at least single digit µM to mM) supports its usage in both analytical measurements where only trace amount of ATP is present and live cell ATP imaging when physiological ATP concentration elevates to ~ 5 mM.

Study with model cell U2OS: the ATP aptamer-based probe senses intracellular ATP and facilitates live cell imaging
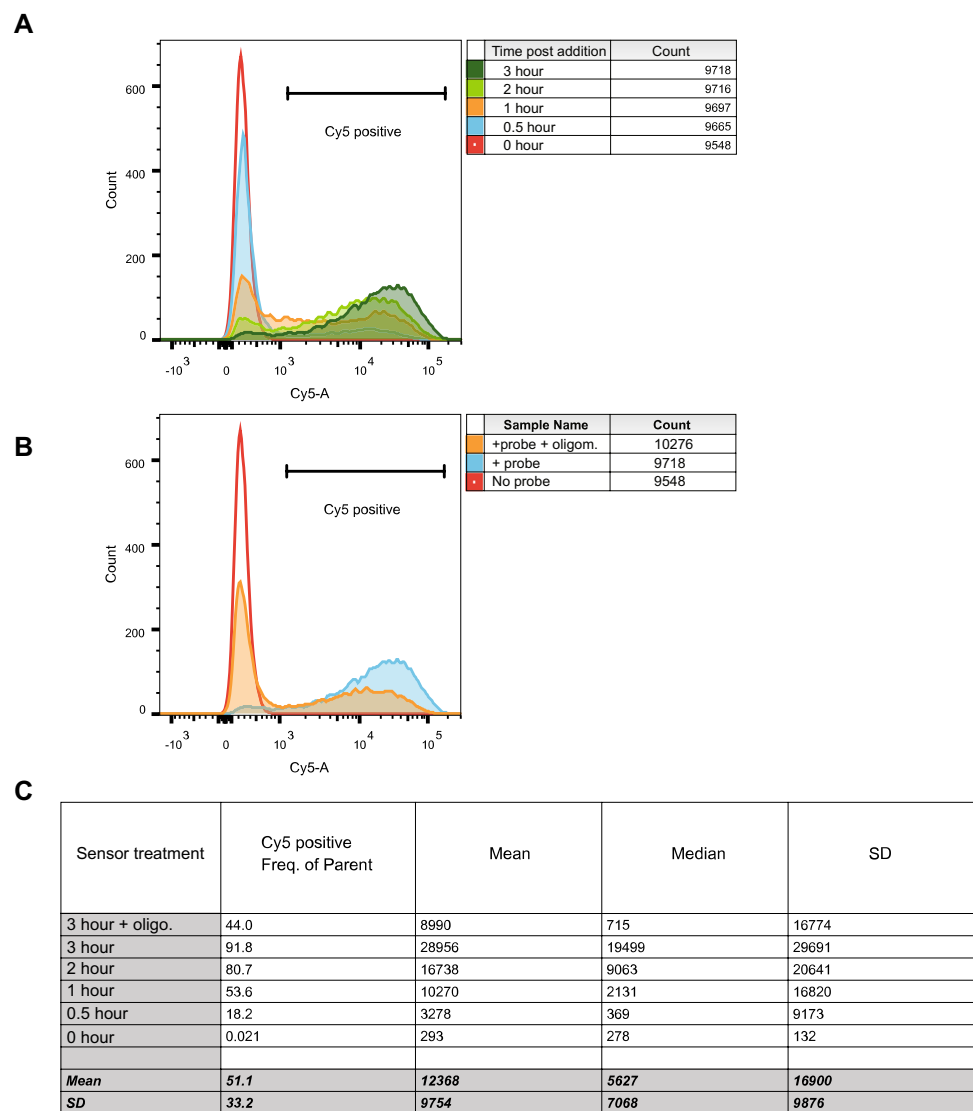
Having demonstrated the signaling ability of the aptamer-based ATP probe in solution, we next tested its ability to detect intracellular ATP. Oligonucleotides do not enter cell actively. One of the widely used strategies to facilitate cellular delivery of oligonucleotides is to use liposome-based carriers as illustrated in Fig. S2. We evaluated a few commercially available liposome acting reagents and determined to use lipofectamine for following studies due to its relatively high efficiency for the probe.

Model cell line U2OS (human bone osteosarcoma) was used to evaluate the entry and performance of the probe. At first, flow cytometry was employed to monitor the emerging of Cy5 positive cell population over a 3-h time course (Fig. 3). An evident shift toward Cy5 positive population was observed at 1 h (53.6%) that reaches 91.8% at 3 h (Fig. 3A and C). To confirm that the release of Cy5 fluorophore inside cells is specific to ATP, we treated cells with oligomycin that blocks ATP synthesis and thus causes depletion of cellular ATP. Addition of oligomycin undermined the release of Cy5 leading to a drop of Cy5 positive population from 91.8 to 44% suggesting that the probe is specific to intracellular ATP concentration (Fig. 3B and C). Two hours was used as standard treatment for following studies. Moreover, efficient cellular uptake by two more cell types HEK-293 and MEF were observed (Fig. S3A and S3B) suggesting wide applicability of this ATP probe for a broad spectrum of cell types.

The capability of sensing intracellular ATP in cellular context is further evaluated. Imaging is the most adoptable approach for sensing of intracellular molecules in live cells. As a result, we evaluated the compatibility and performance of the probe in fluorescent live cell imaging. Perinuclear and cytosolic localization of released Cy5 was observed 2 h after the administration of the probe (Fig. 4A

Fig. 3 Aptamer-based ATP probe senses cellular ATP in U2OS model cell. **A** Time course flow cytometry facilitated profiles of Cy5 release post-lipofectamine-assisted delivery of the probe. Considerable right (Cy5 positive) shift started to occur shortly at 1 h and reached close-to-completion state at 3 h. Two hours is used for all following investigation. **B** The release of Cy5 and fluorescence turn-on was specific to ATP as oligomycin pretreatment largely abrogated the right shift. **C** Statistics of U2OS cell fluorescence at each time points of probe delivery


A

Time post addition	Count
3 hour	9718
2 hour	9716
1 hour	9697
0.5 hour	9665
0 hour	9548

B

Sample Name	Count
+probe + oligom.	10276
+ probe	9718
No probe	9548

C

Sensor treatment	Cy5 positive Freq. of Parent	Mean	Median	SD
3 hour + oligo.	44.0	8990	715	16774
3 hour	91.8	28956	19499	29691
2 hour	80.7	16738	9063	20641
1 hour	53.6	10270	2131	16820
0.5 hour	18.2	3278	369	9173
0 hour	0.021	293	278	132
Mean	*51.1*	*12368*	*5627*	*16900*
SD	*33.2*	*9754*	*7068*	*9876*

(top)), while oligomycin treatment reduced the staining intensity (Fig. 4A (below). ImageJ facilitated quantification of fluorescence (Fig. 4B) suggests a statistically significant diminish with ATP depletion by oligomycin. These data are also in agreement with the flow cytometry experiments (Fig. 3B). In summary, the probe enters the model cells U2OS with high efficiency shortly within 3 h. The probe is live cell imaging compatible and possesses high specificity for intracellular ATP. Moreover, the probe is intrinsically low in cytotoxicity (Fig. S4). Uptaken probes eventually undergo nuclease mediated clearance and metabolization. As cyanine fluorophores is known to possess low toxicity [37], we did observe disappearance of cellular fluorescence over 48 h (data not shown). Unlike nanoparticle mediated delivery which deposits particles to both cells and culture, lipofectamine is considerably cell friendly.

ATP aptamer-based probe assists in characterization and selection of functional cardiomyocyte isolates

U2OS serves as a representative of cultured cells with relatively high homogeneity. Intracellular molecular sensing for extreme cellular/tissue context represents the highest challenge in the field of sensor development. We were prompted to evaluate the sensing performance of the probe in isolated cardiomyocyte culture, a crucial material for cardiac tissue engineering.

Neonatal rat heart was harvested and subject to isolation and selection for cardiomyocytes. After the procedure functional colonies when assessed by spontaneous beating comprises ~20% of the all population (data not shown). Flow cytometry suggested 37.5% Cy5 positive cells after 2 h probe staining (Fig. 5A). The overall elevation of fluorescence was statistically significant (Fig. 5A statistic panel).

Fig. 4 Live cell imaging with the ATP probe. **A** Fluorescence images of ATP probe-stained live cells without (top) or with (below) the treatment of oligomycin (10 µg/mL). Red, ATP probe; green, tubulin (cytosol); blue, Hoechst (nuclei). Cytosolic and perinuclear fluorescence of ATP probe was evidently observed 2 h post the introduction of probe-lipofectamine complex. Specificity of ATP probe was validated with oligomycin treatment (10 µg/mL) which suppressed ATP probe signal. **B** Statistical analysis revealed significant reduction ($p < 0.01$) of ATP probe signal in the oligomycin treated cells. Microscopy fluorescence quantification was carried out with ImageJ. ** denotes significant changes with p value < 0.01 estimated by t-test
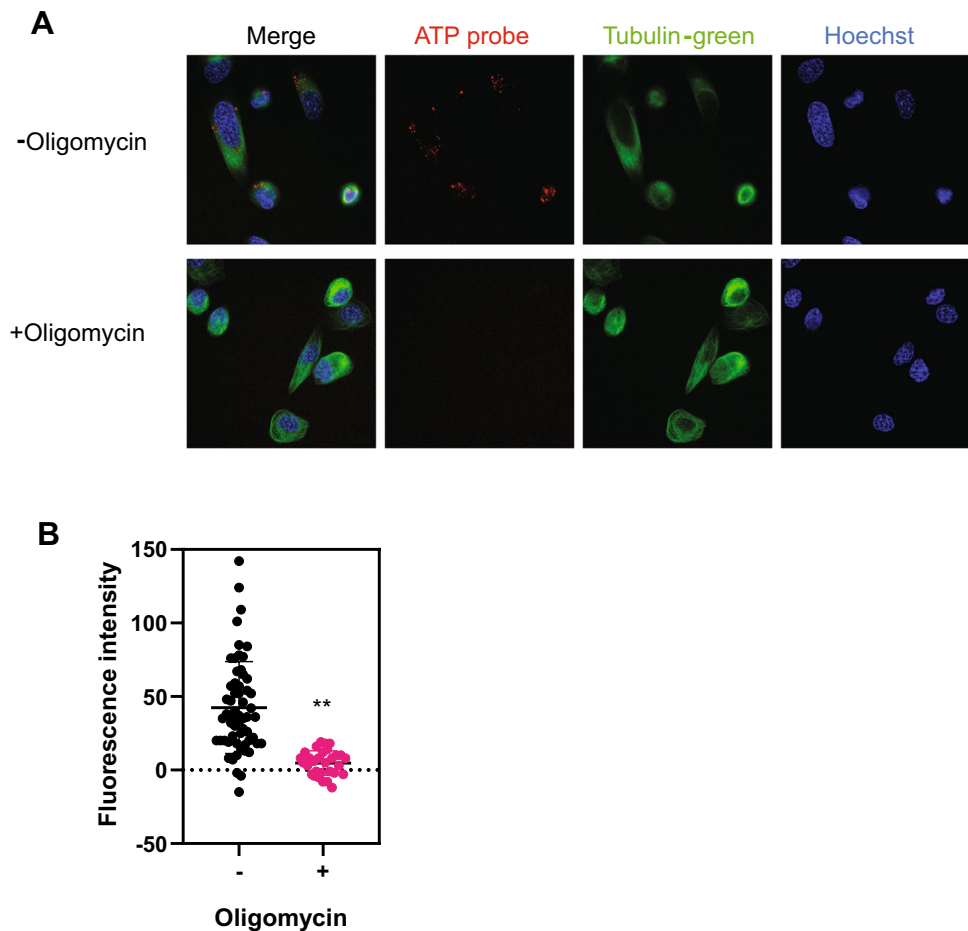
The specificity of the probe was confirmed with reversal (Cy5 positive drops from 37.5 to 15.7%) when given oligomycin mediated ATP depletion (Fig. 5A). The "reduced Cy5 positive population" (37.5%) when compared to U2OS (90.7%) can be attributed to inherent low transfection efficiency of liposome base approaches for selected cell type and reduced viability post the isolation and selection procedure which is also implied by low percentage of functional colonies. Nevertheless, similar cellular staining pattern was observed as in U2OS cells where perinuclear and cytosolic localization was found (Fig. 5B (top)). Consistent with the flow cytometry study, microscopy staining diminishes alongside with the oligomycin treatment suggesting specificity to ATP (Fig. 5B (below)). Moreover, we also documented match between spontaneous beatings of cardiomyocytes with positive staining (Fig. 5C). While the probe is able to enter cultured cardiomyocyte and perform as expected. We believe that a loss of efficiency in cellular delivery does exist and represents the largest limitation of application of the probe in such cellular context. Studies on more appropriate or distinct delivery procedure are on demand. Nevertheless, the probe represents an efficient and alternative approach to characterize fresh cardiomyocyte isolates that could assist

more accurate selection of functional and viable colonies which is crucial for the success of cardiac engineering.

A14 flexible intermolecular link confers regeneration capability

The reporter flare separates from the ATP aptamer when ATP incorporates into the complex. Diffusion of the released chain makes the probe un-reusable. A rationale approach toward regeneration capability is to introduce a linker between the aptamer and reporter flare molecules. A new probe with additional A14 sequence (Fig. 6A) was synthesized. The Cy5 and quencher groups are repositioned for technical hardship in synthetic chemistry. We validated the ATP sensing ability and regeneration capability of the modified probe in solution with ATP depletion by phosphohydrolase apyrase that converts ATP to AMP which is a poor substrate for the ATP aptamer (Fig. 2A).

The modified probe conserves the ATP sensing ability. Addition of 140 µM ATP to 250 nM probe in solution elicits a strong increase in fluorescence (Fig. 6B). However, ATP depletion by apyrase does not render fast turn-over of fluorescence possibly due to a retardant annealing between the

Fig. 5 Application of the ATP probe in the source materials of cardiac tissue engineering, fresh cardiomyocyte isolate. **A** Timely cellular uptake assessed by flow cytometry in newly isolated neonatal rat cardiomyocytes. Statistically significant red shift was observed 2 h after addition of the ATP probe. Oligomycin pretreatment efficiently restrains the red shift. **B** Microscopy images of ATP probe-stained live cardiomyocytes. Red, ATP probe; green, tubulin (cytosol); blue, Hoechst (nuclei). Cytosolic and perinuclear fluorescence of ATP probe was evidently observed 2 h post-introduction of the probe-lipofectamine complex (top). Consistent with the flow cytometry study oligomycin treatment (10 µg/mL) suppresses ATP probe signal in a treatment time dependent manner (below). **C** Fluorescence images of ATP probe-stained live cardiomyocytes. "Beating" is associated with high ATP concentration as indicated by the ATP probe
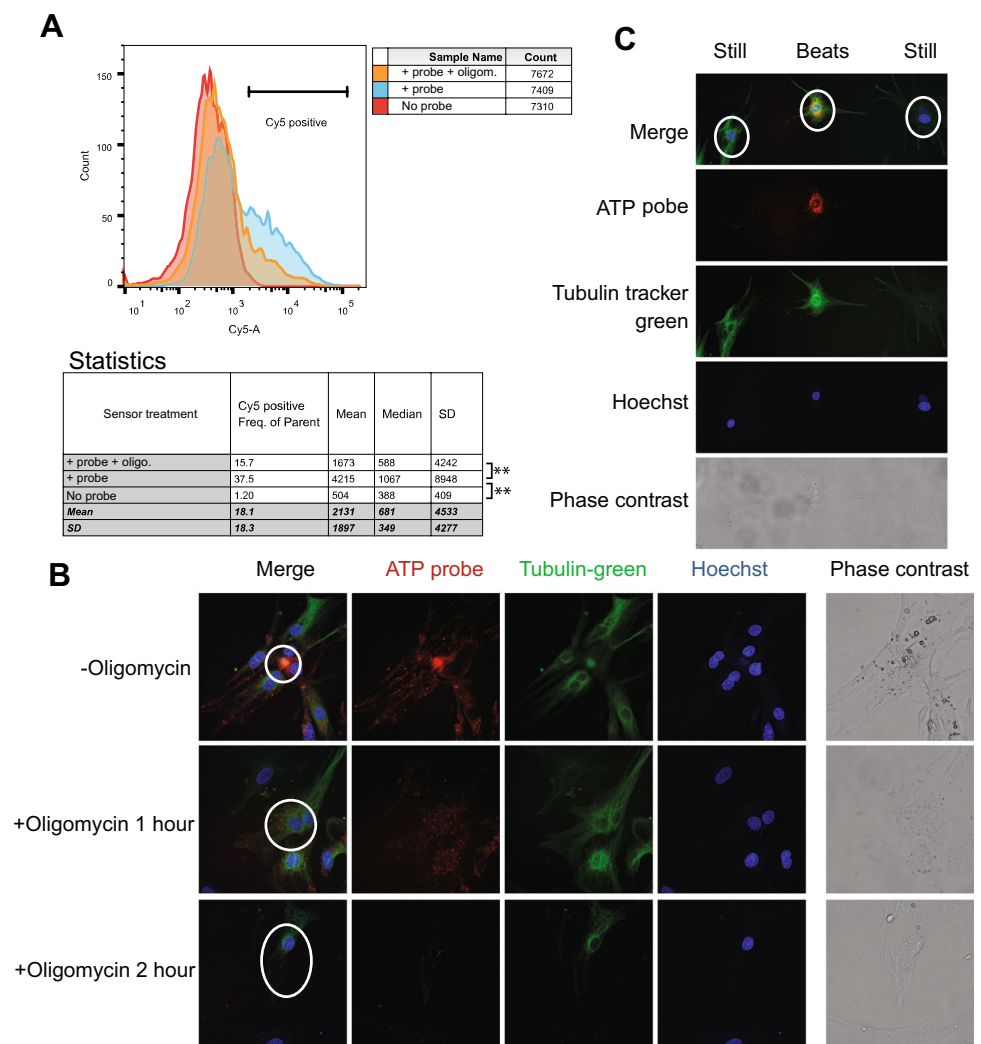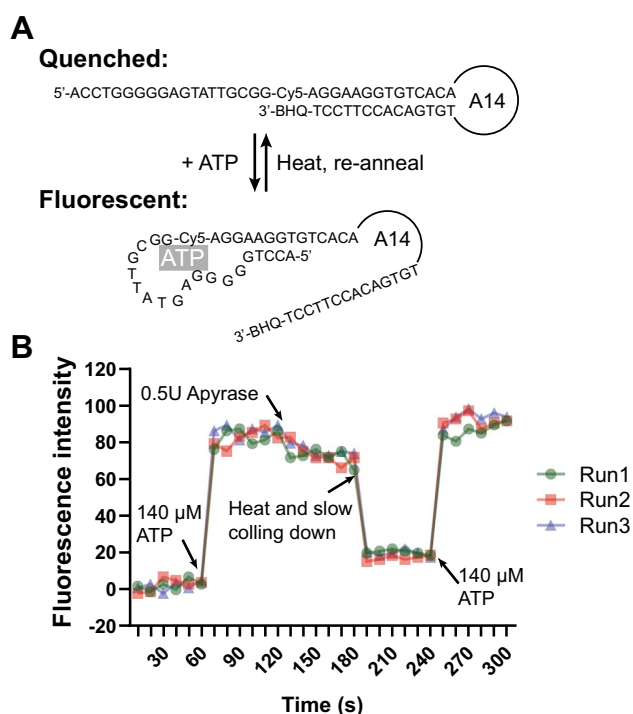

aptamer and reporter chain though the resulting structure theoretically resides thermodynamically more stable. As a result, manned regeneration was given. The calculated melting temperatures (Tm) for the fluorescent and quenched states are calculated as 12 and 42 ˚C respectively. The solution was subject to 70 ˚C, 10 min of incubation, which fully separates the complementary segments, and followed by slow cooling down to room temperature. This allows reanneal and formation of the fluorescence quenched structure as well as inactivation of apyrase activity. Despite a slightly elevated basal fluorescence signal, possibly due to the limited affinity of the probe to AMP, a second addition of ATP induces a pronounced increase in fluorescence (Fig. 6B). These suggest that the new probe configuration with the poly(A) sequence and repositioned fluorophores retains the ATP sensing ability and can be regenerated by simple temperature manipulation.

Introduction of the flexible multiple-adenosine linker between the aptamer and reporter strand restricts the spatial diffusion of the reporter strand post ATP incorporation and makes the probe regeneration compatible. Thorough regeneration relies on temperature manipulation according to our in tube test, which limits the use in a real-time and constant monitoring of ATP changes in solution. Nevertheless, immobilization of the probes on to solid phase could support its use as an on-demand probe such as a multiple-use electrode or a reusable pH strip. It is worth noting that denaturing at 70 ˚C was tested and used instead of more common 95–100 ˚C followed by cooling down. This poses reduced impacts on any further modification to the probe, for example, solid phase immobilization which might be sensitive to high temperature. Meanwhile, to be a long lasting reusable sensing platform, further exploration is indeed needed to improve the stability of the probe in vitro. We propose capsulation of the probe into a small molecular permeable outlayer as a protection from environmental nuclease.

A

Quenched:

5'-ACCTGGGGGAGTATTGCGG-Cy5-AGGAAGGTGTCACA — (A14)
3'-BHQ-TCCTTCCACAGTGT

+ ATP ⇵ Heat, re-anneal

Fluorescent:

(figure A — aptamer probe schematic)

B

Fig. 6 Reversible ATP aptamer probe and its regeneration. **A** A 14 adenosine linker is introduced between the ATP responsive aptamer and reporter flare molecules to form the new reversible probe. Switch between the two fluorescent states is realized by increasing ATP or heat and re-anneal. **B** Functional validation of the new probe is carried out in solution with 250 nM probe and 140 μM ATP. All components are reconstituted in nuclease free water. Comparable fluorescence response is retained by the modified probe. Apyrase mediated hydrolysis of ATP results in limited conversion between the states. Nevertheless, sufficient regeneration can be achieved by 70 °C, 10 min heating and slow cooling down, which inactivates the apyrase activity as well. Considerable fluorescence response is restored by this regeneration protocol as a second ATP addition elicits fluorescence considerably. Note that the lapse on time axis is mostly on scale except for the additions of ATP the step of regeneration when the intervals are omitted and presented as 10 s

Conclusion

We present a new, simple aptamer-based probe that can be used to detect and quantify a small molecule analyte (ATP) in both solution and live cell. The aptamer-based probe is cell friendly and causes limited cytotoxicity as the major components oligonucleotides and cyanine fluorophores can be metabolized by cells. The probe is of high sensitivity to trace level ATP (single digit μM, Fig. 2). Given the advantage of not depending on complex conversion of FRET signal, or quench by large molecules/structures (nanoparticle, nanosheets), the probe is of high versatility as differential formations (probe concentration) could be readily adopted for sensing of ATP at broad range concentrations, from μM to physiologically relevant mM by straightforward changing the probe concentration (Fig. S1) and even higher. With the assistance of lipofectamine, the presented aptamer probe readily enters U2OS cells and is able to directly sense intracellular ATP levels, which makes them well-suited for live cell imaging and sorting studies. In a new rat cardiac isolated which represents a more delicate culture of higher cellular heterogeneity, by sensing intracellular ATP concentration, the probe is able to distinguish functional (beating) colonies. This represents a novel fluorescence-based approach for efficient selection of cardiomyocytes that are the most crucial materials for cardiac tissue engineering.

Code availability Not applicable.

Declarations

Ethics approval All applicable international, national, and/or institutional guidelines for the care and use of animals were followed.

Consent to participate Not applicable.

Consent for publication Not applicable.

Conflict of interest The authors declare no competing interests.

References

1. Shyh-Chang N, Zhu H, Yvanka de Soysa T, Shinoda G, Seligson MT et al (2013) Lin28 enhances tissue repair by reprogramming cellular metabolism. Cell 155(4):778–92. https://doi.org/10.1016/j.cell.2013.09.059

2. Patel A, Malinovska L, Saha S, Wang J, Alberti S et al (2017) ATP as a biological hydrotrope. Science 356(6339):753–756. https://doi.org/10.1126/science.aaf6846

3. McKenney RJ, Huynh W, Tanenbaum ME, Bhabha G, Vale RD (2014) Activation of cytoplasmic dynein motility by dynactin-cargo adapter complexes. Science 345(6194):337–341. https://doi.org/10.1126/science.1254198

4. Wu D, Lee S, Luo J, Xia H, Gushchina S et al (2018) Intraneural injection of ATP stimulates regeneration of primary sensory axons in the spinal cord. J Neurosci 38(6):1351–1365. https://doi.org/10.1523/jneurosci.1660-17.2017

5. Mikolajewicz N, Zimmermann EA, Willie BM (2018) Mechanically stimulated ATP release from murine bone cells is regulated by a balance of injury and repair. 7: https://doi.org/10.7554/eLife.37812

6. Sun D, Junger WG, Yuan C, Zhang W, Bao Y et al (2013) Shockwaves induce osteogenic differentiation of human mesenchymal stem cells through ATP release and activation of P2X7 receptors. Stem Cells 31(6):1170–1180. https://doi.org/10.1002/stem.1356

7. Di Virgilio F, Adinolfi E (2017) Extracellular purines, purinergic receptors and tumor growth. Oncogene 36(3):293–303. https://doi.org/10.1038/onc.2016.206

8. Kasama H, Sakamoto Y, Kasamatsu A, Okamoto A, Koyama T et al (2015) Adenosine A2b receptor promotes progression of human oral cancer. BMC Cancer 15:563. https://doi.org/10.1186/s12885-015-1577-2

9. Amoroso F, Capece M, Rotondo A, Cangelosi D, Ferracin M (2015) The P2X7 receptor is a key modulator of the PI3K/GSK3β/VEGF signaling network: evidence in experimental neuroblastoma. Oncogene 34(41):5240–51. https://doi.org/10.1038/onc.2014.444

10. Yang H, Geng YH, Wang P (2020) Extracellular ATP promotes breast cancer invasion and chemoresistance via SOX9 signaling. 39(35): 5795–5810. https://doi.org/10.1038/s41388-020-01402-z

11. Özilgen M, Yilmaz B (2020) COVID-19 disease causes an energy supply deficit in a patient. Int J Energy Res. https://doi.org/10.1002/er.5883

12. Taghizadeh-Hesary F, Akbari H (2020) The powerful immune system against powerful COVID-19: A hypothesis. Med Hypotheses 140:109762. https://doi.org/10.1016/j.mehy.2020.109762

13. Edwards C (2020) New horizons: does mineralocorticoid receptor activation by cortisol cause ATP release and COVID-19 complications? J Clin Endocrinol Metab. https://doi.org/10.1210/clinem/dgaa874

14. Ribeiro DE, Oliveira-Giacomelli Á (2020) Hyperactivation of P2X7 receptors as a culprit of COVID-19 neuropathology. 1–16. https://doi.org/10.1038/s41380-020-00965-3

15. Yu K, Hai X, Yue S, Song W, Bi S (2021) Glutathione-activated DNA-Au nanomachine as targeted drug delivery platform for imaging-guided combinational cancer therapy. Chem Eng J 22:129535. https://doi.org/10.1016/j.cej.2021.129535

16. Yue S, Li Y, Qiao Z, Song W, Bi S (2021) Rolling circle replication for biosensing, bioimaging, and biomedicine. Trends Biotechnol. https://doi.org/10.1016/j.tibtech.2021.02.007

17. Yue S, Song X, Song W, Bi S (2019) An enzyme-free molecular catalytic device: dynamically self-assembled DNA dendrimers for in situ imaging of microRNAs in live cells. Chem Sci 10(6):1651–1658. https://doi.org/10.1039/c8sc04756a

18. Abe H, Ino K, Li CZ, Kanno Y, Inoue KY et al (2015) Electrochemical imaging of dopamine release from three-dimensional-cultured PC12 cells using large-scale integration-based amperometric sensors. Anal Chem 87(12):6364–6370. https://doi.org/10.1021/acs.analchem.5b01307

19. Zhang L, Su F, Buizer S, Kong X, Lee F et al (2014) A polymer-based ratiometric intracellular glucose sensor. Chem Commun (Camb) 50(52):6920–6922. https://doi.org/10.1039/c4cc01110d

20. Wu S, Wu S, Yi Z, Zeng F, Wu W et al (2018) Hydrogel-based fluorescent dual pH and oxygen sensors loaded in 96-well plates for high-throughput cell metabolism studies. Sensors (Basel):18(2). https://doi.org/10.3390/s18020564

21. Li C, Numata M, Takeuchi M, Shinkai S (2005) A sensitive colorimetric and fluorescent probe based on a polythiophene derivative for the detection of ATP. Angew Chem Int Ed Engl 44(39):6371–6374. https://doi.org/10.1002/anie.200501823

22. Middleton DA, Hughes E, Esmann M (2011) The conformation of ATP within the Na, K-ATPase nucleotide site: a statistically constrained analysis of REDOR solid-state NMR data. Angew Chem Int Ed Engl 50(31):7041–7044. https://doi.org/10.1002/anie.201100736

23. Fu C, Fang Y, Song L (1999) Determination of adenosine phosphate by co-electroosmotic capillary electrophoresis with amperometric detection. Anal Chim Acta 399(3):259–263

24. Wang J, Wang LH, Liu XF, Liang ZQ, Song SP et al (2007) A Gold Nanoparticle-Based Aptamer Target Binding Readout for ATP Assay. Adv Mater 19(22):3943–3946

25. Lee DH, Kim SY, Hong JI (2004) A fluorescent pyrophosphate sensor with high selectivity over ATP in water. Angew Chem Int Ed Engl 43(36):4777–4780. https://doi.org/10.1002/anie.200453914

26. Perez-Ruiz T, Martinez-Lozano C, Tomas V, Martin J (2003) Determination of ATP via the photochemical generation of hydrogen peroxide using flow injection luminol chemiluminescence detection. Anal Bioanal Chem 377(1):189–194. https://doi.org/10.1007/s00216-003-2071-2

27. Nakano S, Mashima T, Matsugami A, Inoue M, Katahira M et al (2011) Structural aspects for the recognition of ATP by ribonucleopeptide receptors. J Am Chem Soc 133(12):4567–4579. https://doi.org/10.1021/ja110725d

28. Du Y, Chen C, Zhou M, Dong S, Wang E (2011) Microfluidic electrochemical aptameric assay integrated on-chip: a potentially convenient sensing platform for the amplified and multiplex analysis of small molecules. Anal Chem 83(5):1523–1529. https://doi.org/10.1021/ac101988n

29. Xu JP, Song ZG, Fang Y, Mei J, Jia L et al (2010) Label-free fluorescence detection of mercury(II) and glutathione based on Hg2+-DNA complexes stimulating aggregation-induced emission of a tetraphenylethene derivative. Analyst 135(11):3002–3007. https://doi.org/10.1039/c0an00554a

30. Wang L, Chen W, Ma W, Liu L, Ma W et al (2011) Fluorescent strip sensor for rapid determination of toxins. Chem Commun (Camb) 47(5):1574–1576. https://doi.org/10.1039/c0cc04032k

31. Zhao S, Yang W, Lai RY (2011) A folding-based electrochemical aptasensor for detection of vascular endothelial growth factor in human whole blood. Biosens Bioelectron 26(5):2442–2447. https://doi.org/10.1016/j.bios.2010.10.029

32. Iliuk AB, Hu L, Tao WA (2011) Aptamer in bioanalytical applications. Anal Chem 83(12):4440–4452. https://doi.org/10.1021/ac201057w

33. Zhang H, Zhou L, Zhu Z, Yang C (2016) Recent progress in aptamer-based functional probes for bioanalysis and biomedicine. Chemistry 22(29):9886–9900. https://doi.org/10.1002/chem.201503543

34. Sun W, Song W, Guo X, Wang Z (2017) Ultrasensitive detection of nucleic acids and proteins using quartz crystal microbalance and surface plasmon resonance sensors based on target-triggering multiple signal amplification strategy. Anal Chim Acta 978:42–47. https://doi.org/10.1016/j.aca.2017.04.047

35. Suzuki Y, Yokoyama K (2015) Development of functional fluorescent molecular probes for the detection of biological substances. Biosensors (Basel) 5(2):337–363. https://doi.org/10.3390/bios5020337

36. Terai T, Nagano T (2013) Small-molecule fluorophores and fluorescent probes for bioimaging. Pflugers Arch 465(3):347–359. https://doi.org/10.1007/s00424-013-1234-z

37. Shi C, Wu JB, Pan D (2016) Review on near-infrared heptamethine cyanine dyes as theranostic agents for tumor imaging, targeting, and photodynamic therapy. J Biomed Opt 21(5):50901. https://doi.org/10.1117/1.JBO.21.5.050901